TOWARD SELF-CONSISTENT-FIELD MODELS OF THE MOON AFTER THE FORMATION IMPACT . D. G. Korycansky, *CODEP, Department of Earth and Planetary Sciences, University of California, Santa Cruz CA 95064* .

Introduction

In recent years, the canonical picture of the most widely-accepted scenario of the Moon's formation (the giant impact theory) has become complicated due to recent high-precision measurement of isotope ratios for oxygen and other elements in lunar samples. The measurements suggest that the bulk isotope ratios for the Moon are essentially identical to those of the Earth (e.g. Zhang *et al.* 2012). This is a problem for the "classic" scenario in which the Moon is formed by the oblique impact of a Mars-mass body with the proto-Earth and subsequent accretion from a post-impact disk surrounding the Earth. The classic picture suggests that the Moon is primarily made of impactor material. Generating near-identical isotope ratios by this sequence of events would require a presumably unlikely near-identical isotopic composition of the impactor and proto-Earth.

Thus, new models have been proposed that may overcome this difficulty. In particular, Ćuk and Stewart (2012) proposed a model in which the proto-Earth is rapidly spinning and struck by a relatively low-mass impactor, forming a hot, rapidly rotating structure in which convection allows effective mixing and homogenization of isotope ratios for the subsequently formed Moon. The type of post-impact structure has been dubbed a "synestia" by Lock et al. (2017, 2018).

The Self-Consistent Field method

The work described here is part of a larger effort to validate formation models via high resolution simulations the Moon-forming impact with a state-of-the-art hydrodynamics code. While such a calculation is the best method available for describing the impact and its immediate aftermath, it is limited to modeling a time period of hours to several days after the impact. Studying the longer-term evolution of the Earth-Moon system will require a different method that sacrifices some of the dynamical details of the system in order to model quasi-steady-state long-term development. We have been working on applying the so-called Self-Consistent Field (SCF) method in order to generate post-impact configurations. The SCF method has a long pedigree in astrophysics stretching back to the 1960s, having been applied to modeling self-gravitating bodies with significant angular momentum (Tassoul 1979). In particular it is applicable to the "in-between" situation where objects neither rotate slowly enough to be considered quasi-spherical, or so fast as to be approximated by thin disks (as in accretion disk theory).

Use of the method requires the assumption of a configuration in which 1) the rotation rate Ω is a function of the cylindrical radius r and the concomitant assumption that the pressure P and density ρ can be related by $P = P(\rho)$, i.e. that the configuration is barotropic (even if the underlying equation

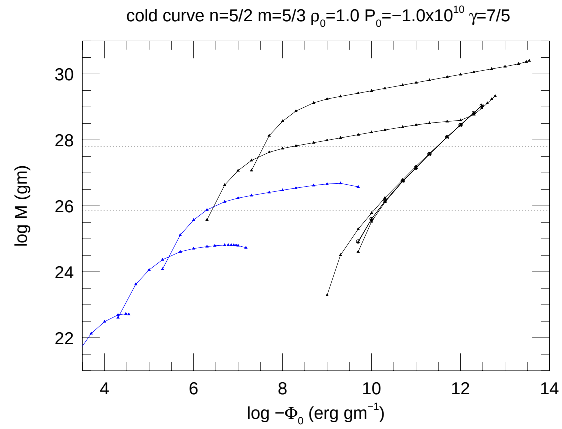

Figure 1: Mass-potential relation for cold-curve EOS with parameters as indicated. Successive curves from bottom up indicate values of $K' = 10^8$, 10^9, 10^{10}, 10^{11}, 10^{12}, 10^{13}. Blue curves (for $K' = 10^9$, 10^{10}, 10^{11}) indicate low-density branches of enthalpy curves that have double positive-slope regions. The horizontal dashed lines indicate one lunar mass (7.4×10^{25} gm)) and one Earth mass 6.4×10^{27} gm).

of state (EOS) is more general (i.e. $P = P(\rho, T)$). (For example, if the configuration is isentropic, or more generally, the temperature T also happens to be a function of ρ in the object.) If these assumptions hold, then the gravitational potential can be algebraically related to the enthalpy $H = \int dP/\rho = H(\rho)$ and the configuration structure can be calculated by an iterative procedure involving the solution of the Poisson equation for successive iterations of the object's density structure $\rho(r,z)$. Such a method was developed in the 1960s and has been applied to idealized configurations (e.g. rapidly rotating polytropes) and models of rapidly rotating stars. We developed a program for SCF calculations and have tested it successfully on configurations such as rotating polytropes (cf. James 1964).

Isentropes and enthalpies for non-ideal gases

For post-Moon-forming impact models, an additional requirement is a realistic equation of state, such as the tabular SESAME EOS, or the semi-analytic ANEOS (Melosh 2007). We acquired the ANEOS routines and input files for materials of interest, such as SiO_2 and dunite, and have generated enthalpy tables $H(\rho)$ for (e.g.) isentropes.

The enthalpy H is written as $E + PV$ and for isentropes is equivalent to $H = \int dP/\rho$. For substances of interest $P(\rho)$ and its differential $dP(\rho)$ can be negative in certain parameter regimes, typically at low temperatures and pressures (which may or may not be of physical interest). The negative portions can in turn generate entropies that are non-monotonic functions of ρ for some values of entropy S. These regions of parameter space are not suitable for modeling, but portions of the enthalpy curve can be used to make either low- or high-density models over a more limited range of ρ.

To understand the properties of configurations composed of non-ideal materials (e.g. SiO_2 or H_2O), we have temporarily stepped back to investigate non-rotating (spherical) configurations. We integrate Poisson's equation in spherical symmetry with the link between density and potential provided by the enthalpy $H(\rho) = -(\Phi + \Phi_0)$, where Φ_0 is a constant of integration that sets the mass of the configuration, yielding a second-order non-linear ordinary differential equation for the potential $\Phi(r)$

$$\frac{1}{r^2}\frac{d}{dr}\left(r^2\frac{d\Phi}{dr}\right) = 4\pi G\rho(\Phi). \qquad (1)$$

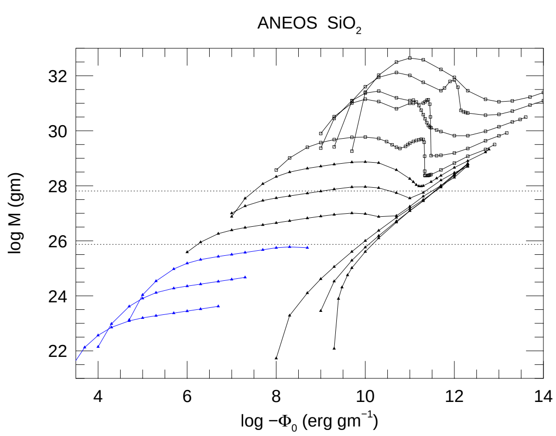

Figure 2: Mass-potential relations for ANEOS SiO_2 with different values of entropy. Successive curves indicate entropy values of $S = 4\times10^{11}$, 5×10^{11}, 6×10^{11}, 7×10^{11}, 8×10^{11}, 9×10^{11}, 1.0×10^{12}, 1.2×10^{12}, 1.5×10^{12}, 2.0×10^{12}, 2.5×10^{12} erg gm^{-1}. As in Fig. 1, Blue curves (for $K' = 4\times10^{11}$, 5×10^{11}, 6×10^{11} erg gm^{-1}) indicate low-density branches of enthalpy curves that have double positive-slope regions. The horizontal dashed lines indicate one lunar mass and one Earth mass.

Analytic "Cold Curve" EOS

ANEOS is something of a "black box", and we have found it helpful to also work with an analytic approximated equation of state based on the discussion in Melosh's 2007 paper. This "cold curve" EOS is given by

$$P = P_T + P_c = (\gamma-1)\rho e + K(\eta^n - \eta^m), \quad \eta = \rho/\rho_0 \qquad (2)$$

where $n > m$ so that $P_c \to 0$ as $\rho \to 0$. Using the first law of thermodynamics $de + PdV = 0$ (with $V = 1/\rho$) we can solve for the energy along an adiabat

$$e = \frac{K}{\rho_0}\left[\frac{\eta^{n-1}}{n-\gamma} - \frac{\eta^{m-1}}{m-\gamma}\right] + K'\rho^{\gamma-1}, \qquad (3)$$

where K' is a constant of integration labeling the entropy. The corresponding enthalpy $H = e + PV$ is

$$H = e + \frac{P}{\rho} = \frac{K}{\rho_0}\left[\frac{n\eta^{n-1}}{n-\gamma} - \frac{m\eta^{m-1}}{m-\gamma}\right] + \gamma K'\rho^{\gamma-1}. \qquad (4)$$

Integration of spherical models

Integration is performed by setting the initial condition $\Phi = \Phi_0$ at $r = 0$ and integrating eqn 1 outwards to the point R where $\Phi = 0$. Figure 1 shows the run of mass versus central potential for successive values of thermal parameter K'. Figure 2 shows the runs of mass vs. central potential for ANEOS SiO_2 configurations. An ideal gas ($P = K'\rho^\gamma$) has power-law (polytropic) behavior for $M(\Phi_0) \propto \Phi_0^{(3\gamma-4)/2(\gamma-1)}$ so the non-power-law and non-monotonicity for both EOSes show the effects of non-ideal-gas material. For example, non-monotonic curves of $H(\rho)$ give rise to low-density (and thus low-mass) branches of the mass-potential curves as indicated in Figs 1 and 2. Curves for which M is a decreasing function of Φ_0 (equivalent to $n > 3$ polytropes) indicate potentially dynamically unstable configurations.

Acknowledgments

This work was supported by NASA Emerging Worlds Program award 80NSSC18K0499.

References

Zhang *et al.* 2012 *Nature Geophys.* **5**, 251.
Ćuk, M. and Stewart, S. T. 2012 *Science* **338**, 1047.
Lock, S. and Stewart, S. T. 2017 *J. Geophys. Res* 122, 950.
Lock, S. *et al.* 2018 *J. Geophys. Res* **123**, 910.
Tassoul, J. 1979 *Theory of Rotating Stars*, Princeton University Press.
James, R. A. 1964 *Astrophys. J.* **140**, 552.
Melosh, H. J. 2007 *Met. Plan. Sci.* **42**, 2079.